Nuclear Instruments and Methods in Physics Research A 387 (1997) 305–314

NUCLEAR INSTRUMENTS & METHODS IN PHYSICS RESEARCH Section A

ELSEVIER

Generation of sub-picosecond electron bunches from RF photoinjectors

L. Serafini[a], R. Zhang[b,*], C. Pellegrini[b]

[a]*INFN – Milan, Via Celoria 16, 20133 Milan, Italy*
[b]*Department of Physics, UCLA, Los Angeles, CA 90024, USA*

Received 19 April 1996; revised form received 15 November 1996

Abstract

In this paper we discuss the possibility to generate sub-picosecond electron bunches directly from a photoinjector by illuminating a photo-cathode in an RF cavity with a phase-locked sub-picosecond laser pulse. In particular, we address all de-bunching effects taking place during acceleration and transport through a photoinjector. We provide analysis of the beam dynamics, as well as the comparison with numerical simulations. The possible performances of the present SATURNUS linac setup are presented, as well as the anticipated capabilities of a multi-cell RF gun structure based on the PWT linac presently in operation at UCLA.

1. Introduction

Sub-picosecond electron pulses have many scientific and industrial applications. They can be used to study molecular dynamics, or to produce ultra-short X-ray pulses for crystallography. Plasma accelerators, such as the Plasma Beat Wave Accelerator (PBWA) [1,2], requires injectors which can generate electron bunches with a length of about 20 to 30 μm, about one tenth of the typical plasma wave wavelength, since the accelerated beam emittance and energy spread scale critically with the ratio of the bunch length of the injected beam to the plasma wavelength. Therefore, the production of high quality and sub-picosecond electron bunches is a critical requirement for plasma accelerators, or, indeed, for any high frequency accelerators.

There are basically three methods to generate sub-picosecond electron bunches. One, the strong bunching method, such as an FEL, able to produce longitudinal focusing and hence to induce bunching or decrease the bunch length. Another method, the weak bunching method, obtains short bunches by a phase space rotation, in a drift space, of a beam which has been previously modulated in energy. Alternatively, one can produce an electron bunch at a photo-emissive surface, with just the required time structure, by using a sub-picosecond laser pulse. In this case one must control that this time structure is not significantly perturbed by the de-bunching effects occurring during the acceleration to relativistic energies. Several weak bunching systems have already been tested experimentally, and some others are under study and/or development. A scheme based on the use of an RF gun followed by magnetic compressors of various kinds has been used by several groups. For example, the production of 100 fs electron bunches by means of a thermoionic RF gun followed by an Alfa-magnet compressor has been recently [3] demonstrated at Stanford. Unfortunately, the normalized transverse emittance obtained with this system, about 40 mm-mrad, is too large for many applications where high quality electron beams are needed, as in Free Electron Lasers. The possibility of obtaining simultaneously a short bunch and a small emittance has been studied [4] with computer codes like PARMELA [5], showing the possibility of acceleration of a 1-ps electron beam through a $1\frac{1}{2}$-cell RF gun operated at 2.856 GHz, boosted by an 8-cell PWT linac to an energy of 16 MeV, then reduced to 80 μm rms bunch length (FWHM) in a magnetic compressor, with an excellent final rms normalized emittance of 0.5 mm-rad.

The plasma-klystron is another weak bunching system proposed recently [6], based on the concept of the Plasma Beat Wave Accelerator. A Langmuir wave is excited in a thin ionized gas jet, and is used to modulate the energy of a 10 MeV electron beam which crosses the gas jet, co-propagating with the laser beat wave pulse. The gas jet is followed by a drift space where the bunching occurs. Preliminary simulations show that a plasma klystron might produce a train of 30 μm long bunches, spaced 300 μm apart, after a 30 cm drift space downstream the gas jet.

* Corresponding author. Tel.: +1 310 206 5584; fax: +1 310 206 1091.

PII S0168-9002(96)01218-1

Another example of weak bunching device is based on the combination of an RF gun working in a strong phase compression regime [7], with a wiggler used as a dispersive device, to transform the energy chirping induced in the beam from the gun, in a bunch length decrease, down in the range of 30 μm.

Typical strong bunching devices are the ones using the FEL interaction occurring inside an undulator between the electron beam and an intense EM wave: the resulting ponderomotive potential well is responsible for a strong coherent bunching of the beam at the wavelength of the radiation field. The simulations of an oscillator-amplifier FEL scheme [8], indicate that a 21 MeV beam with an input current of 150 A can be nicely bunched on the scale of 100 μm radiation wavelength. However, the bunching is quite remarkable in the head part of the electron bunch but somewhat poor in the bunch tail region, due to the slippage effect; these can be eliminated by operating the FEL in a wave-guide, to reduce the group velocity of the radiation near to the beam velocity.

Another FEL based scheme, the adiabatic buncher [9], achieves an adiabatic trapping of particles in the ponderomotive potential well created by a powerful (10 GW) input signal, by using a tapered undulator. The tapering enhances greatly the trapping efficiency, up to almost 90%, as well as reduces by a significant amount (a factor 3) the energy spread at the output. One of the drawbacks of such a scheme is the need of a high power input signal, which prevents its exploitation in the sub-millimeter wavelength region.

In this paper we analyze what is the possible performance of a system based on the last alternative, that is the direct production and acceleration of a sub-picosecond bunch in a photoinjector, illuminating the photo-cathode in the RF gun with a short laser pulse [10]. Assuming the existence of ultra-fast photo-cathodes (response time $\leq$50 fs), we will discuss the beam dynamics in an RF gun driven by a 166 fs (FWHM) laser pulse, mainly in terms of the length of the produced electron bunch. Two main effects, limiting the minimum bunch length attainable with such a scheme, will be discussed in detail: the coupling of the transverse betatron motion with the longitudinal one, inducing a cup-like shaping of the bunch, and the longitudinal space charge field causing a bunch core lengthening. By carefully optimizing the cathode spot size as well as the injection phase one can minimize such effects: simulations show that 50 μm long electron bunches can be produced, assuming zero cathode response time, as far as one takes advantage of the phase compression mechanism.

RF photo-injectors for generating sub-picosecond pulses are well within the present state of the art. After more than a decade of development, tremendous progress has been made in the photoinjector technology [11]. Therefore, it is very appealing to produce sub-picosecond electron pulses by using this method. On the other hand, the beam dynamics of an ultra-short bunch has unique features, which are usually negligible for a long bunch. The RF gun design must be tailored to preserve the laser time structure during acceleration and transport of the beam. Several factors, such as cathode emission delay, finite beam radius, and longitudinal self-field can cause electron bunch lengthening in a photoinjector. To avoid significant lengthening in the tail of the emitted electron bunch the photo-emission must be really prompt, i.e. the photocathode must respond to the laser pulse within times no longer than 20–30 fs. An R&D activity is in progress at UCLA [12], on the prompt photo-emission from bulk and/or thin Mg or Cu films, aimed at understanding whether such response time can be achieved with metallic cathodes, eventually using back illumination of thin films.

The beam dynamics related to bunch lengthening is studied in this paper. In Section 2, we analyze the bunch lengthening in rf photoinjectors, including both single particle and collective effects. In Section 3, we present the simulation results for two different configurations, one based on a $1\frac{1}{2}$-cell gun followed by a linac, the other in a multi-cell gun.

2. Beam dynamics for ultra-short bunch in RF photoinjectors

In this paper we assume that there is no significant delay in the photo-emission processes at the cathode surface, and we minimize all the bunch lengthening effects that may take place during the acceleration through the gun, transport along the beam line, and injection into the interaction area of experiments. In this section we discuss the beam dynamics effects which can lead to bunch lengthening:

(1) single particle dynamics effects, due to the non-isochronous properties of the accelerating RF field;
(2) collective beam dynamics effects, due to space charge.

The main investigation is concentrated here on the acceleration through the RF gun and the booster linac, assuming a straight line injection into the interaction area. The additional bunch lengthening produced by a possible transport line in between deals with the actual design of such a line.

2.1. Single-particle beam dynamics

There are two aspects that induce bunch lengthening effects in single particle beam dynamics: the finite transverse momentum and the finite beam radius. The two factors can be incorporated into a single treatment as far as the parallel component, β_z, of the particle velocity is considered to evaluate the variation of the time of flight between the reference electron (emitted on-axis at the cathode surface) and an electron emitted off-axis at a position r_0, when they travel from the cathode surface up to the RF gun exit.

For the sake of simplicity and without losing generality, we make the following assumptions [13]: the initial transverse momentum of the electrons emitted from the cathode is negligible with respect to the transverse momentum acquired from the transverse RF field forces along the trajectory in the gun; the beam flow is laminar, so that off-axis electrons never cross the axis, and the second order transverse momentum induced by the RF ponderomotive focusing effect is negligible with respect to the first order one, which is given by (in units of mc)

$$p_r = \gamma' r_0 \cos(kz + \phi) \sin(kz)/\sin(\phi) \tag{1}$$

where $k = 2\pi/\lambda_{RF}$, λ_{RF} is the RF wavelength.

The accelerating field in the gun has a peak amplitude E_0 at the cathode. We assume that the electron kinetic energy increases linearly with the distance z from the cathode surface, i.e. $\gamma = 1 + \gamma' z$ with $\gamma' = eE_0/(2mc^2)$. It is usual to introduce the dimensionless quantity α, defined as $\alpha = \gamma'/k$, which is typically ranging between 1/2 and 4 [7]. Eq. (1) is derived under a ballistic approximation which assumes that electrons leave the cathode surface at $v = c$ with a phase ϕ shifted from the actual injection phase ϕ_0 by an amount [14] $\phi = \phi_0 + 1/(2\alpha \sin\phi) + 1/6(\alpha \sin\phi)^2$. The motion is treated, therefore, as relativistic. Since we neglect the second-order ponderomotive force, the off-axis position of an electron in the bunch is only slightly changed with respect to the starting position r_0 at the cathode surface. The longitudinal component β_z of the electron velocity is therefore reduced by an amount:

$$\Delta\beta_z = -r'^2/2 = -(p_r/p_z)^2/2 = -(p_r/\gamma)^2/2 \tag{2}$$

The off-axis electrons will slightly slip toward the bunch tail and the bunch will become cup-shaped: by simply integrating the effect of such a slippage along the acceleration through the gun we find the total slippage ΔL_s:

$$\Delta L_s = -\frac{1}{2}\int_1^{\gamma_f} \frac{p_r^2}{\gamma'\gamma^2}\,d\gamma \tag{3}$$

where γ_f is the electron γ at the gun exit. The maximum slippage will correspond to the electron emitted at the maximum laser spot size R, i.e. when $r_0 = R$. In this case ΔL_s represents the total bunch lengthening. A simplified expression for the relative change δ_s of the bunch length, i.e. $\delta_s = |\Delta L_s|/L_0$ (L_0 is the laser pulse length), can be derived as [7]:

$$\delta_s = \frac{AkR}{\pi}[(0.12 + 0.068\phi)\alpha - 0.035(1 - 0.1\phi)\alpha^2 + 0.1 - 0.026/\alpha]\arctan[(\gamma_f - 2)^{4/5}] \tag{4}$$

δ_s is plotted in Fig. 1 with $\gamma_f = \infty$ for a typical bunch aspect ratio $A = 10$ ($A \equiv R/L_0$) and $kR = 0.06$ for the dimensionless bunch radius (which corresponds to $R =$ 1 mm at $f_{RF} = 2.856$ GHz). The relative bunch lengthening

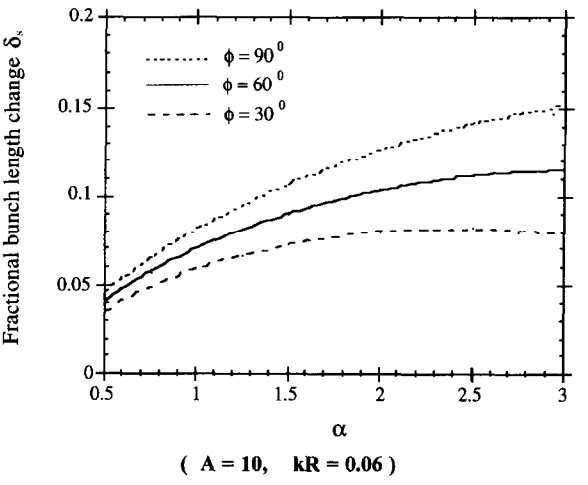

Fig. 1. The relative change of bunch length at different α for $A = 10$ and $kR = 0.06$.

δ_s is confined within 20% in the range of $0.5 < \alpha < 3$ and for phases ranging from 30° to 90° RF phase.

It is interesting to notice that Eq. (4) predicts a total slippage of 12 μm for a bunch with $R = 1$ mm and $L_0 =$ 50 μm, accelerated in a S-band RF gun operated at $E_0 =$ 100 MV/m (for which $\alpha = 1.64$) at $\phi = 90°$ RF phase. Such a slippage, usually negligible for standard operation (a few ps long electron bunch extracted), becomes a relevant problem in this regime of sub-pico-second bunch production.

In most RF guns an external solenoid lens is used, to focus the beam via the applied magneto-static field. This again induces a transverse component β_φ in the electron velocity, given by $\beta_\varphi = (e/2mc)B_0 r_0/\gamma$, where B_0 is the amplitude of the solenoid field. Assuming a constant B_0 field in the first cells of the RF gun, the same integration performed as in Eq. (1) gives the total induced slippage $\Delta L_b = (e/mc)^2 (B_0 r_0)^2/8\gamma'$. Again, applying a 1.5 kG B_0-field in a S-band RF gun operated at 100 MV/m will produce a slippage $\Delta L_b = 10$ μm for an electron emitted at $r_0 = 1$ mm.

These predictions on the two slippage effects, which both produce a cup-shaped curvature of the electron bunch, are nicely confirmed by the numerical simulations, as shown below in the following section. One should, however, recall that the previous analysis takes into account only linear transverse components of the RF field. In case of significant amplitudes of higher spatial harmonics in the RF field on-axis distribution, the non-linear transverse components can significantly perturb the single particle beam dynamics [14] as well as the slippage of off-axis electrons.

There are at least two possible cures for this effect: either the laser pulse or the cathode surface can be shaped in such a way to compensate the electron bunch curvature. In the first case the laser pulse should hit the cathode with

a concave shape, so that the off-axis electrons are emitted before the on-axis ones. The laser pulse curvature C_1 in the (r, z) plane is given actually by

$$C_1 = (k/\pi)[(0.12 + 0.068\phi)\alpha - 0.035(1 - 0.1\phi)\alpha^2 + 0.1 - 0.026/\alpha] \arctan[(\gamma_f - 2)^{4/5}]$$

C_1 is also the coefficient relating the bunch lengthening ΔL_s and the bunch radius squared R^2 in Eq. (4). Typical values for C_1 imply a bending of a few tens of microns for a 1 mm laser spot size. Such a laser pulse shaping has already been performed and tested at Argonne [15] on the scale of 30 ps laser pulses. It needs to be proved that the same technique may be applied on 100 fs pulses. In the latter case, the cathode surface may be shaped according to $-C_1/2$, i.e. with a concave shape, such that off-axis electrons are emitted first and, at the same time, at a greater z than on-axis electrons (emitted at $z = 0$). In this case one should check that the perturbation on the RF field spatial distribution induced by the cathode shaping does not spoil, by introducing higher spatial harmonics, the compensation. Moreover, the cathode curvature also fixes the operating point of the RF gun (i.e. α and ϕ), where the compensation is achieved, with some lacking of flexibility.

2.2. Space charge effects

Another important source of bunch lengthening is due to the longitudinal self-field of the electron bunch, which tends to push the electrons in the bunch head, decelerating the ones in the bunch tail at the same time. During the photo-emission process the strong interaction between the bunch and its image charge on the metallic wall of the cathode further enhances this effect. In order to evaluate the total lengthening occurring up to the gun exit we will assume that the effect is a perturbative one and the electron bunch is produced instantaneously at the cathode location ($z = 0$) with no interaction with the cathode wall [16].

Taking the longitudinal space charge field of a uniform charged cylinder of radius R and length L, carrying a total charge Q and moving along the z-axis with a kinetic energy $T = (\gamma - 1)mc^2$, we evaluate the field value E_z at the bunch head on axis (i.e. $r = 0$ and $z = L_0/2$),

$$E_z = Q[1 + A/\gamma - \sqrt{1 + A^2/\gamma^2}]/(2\pi\varepsilon_0 R^2) \tag{5}$$

where A is the bunch aspect ratio $A = R/L_0$.

In the usual operating range of RF guns, E_z is much smaller than the applied RF field at the cathode. Moreover, since we are considering the regime of high aspect ratio bunches ($A \gg 1$ since $L_0 \approx 50\,\mu$m), the behavior of the longitudinal space charge field shifts from a surface charge regime ($A/\gamma \gg 1$, $E_z \propto Q/R^2$), in the first cell of the gun, toward a linear charge regime ($A/\gamma \ll 1$, $E_z \propto Q/(\gamma R L_0)$) at the gun exit, in case the gun is long enough to enter this regime. The total bunch lengthening ΔL_{sc} can be computed [7] taking into account the energy spread induced by such a longitudinal space charge field and integrating along the acceleration

$$\Delta L_{sc} = \frac{4Qc}{I_A \gamma'^2 R^2} f(A, \gamma_f) \tag{6}$$

where I_A is the Alfven current, Q the bunch charge, and

$$f(A, \gamma_f) = \left\{ \begin{array}{l} A(1 - 1/\gamma_f) + \sqrt{1 + A^2/\gamma_f^2} + (1 - A)\log\left[\dfrac{\gamma_f}{1 + \gamma_f}\right] \\ + A[\operatorname{arcsinh}[A] - \operatorname{arcsinh}[A/\gamma_f]] - \log[2](A - 1) \\ - \sqrt{1 + A^2} \\ \times \left(1 + \log\left[\dfrac{A^2(1 + \gamma_f)}{A^2 - \gamma_f + \sqrt{1 + A^2}\sqrt{1 + A^2/\gamma_f^2}}\right]\right) \end{array} \right\}$$

Actually, ΔL_{sc} represents the increase of the total bunch length for a uniformly charged bunch: since the usual time intensity distribution of the laser pulse is Gaussian, we adopt the increase of the rms length as a prediction for the bunch lengthening of Gaussian bunches. The rms length of a uniform bunch is $L_0/\sqrt{3}$: this should be equated to 2σ rms length of a Gaussian bunch. Therefore, once the rms length of the Gaussian bunch is fixed, the equivalent uniform bunch must have a total length L_0 which is $\sqrt{3}$ times longer. The increase of the rms bunch length, ΔL_{sc}^{2rms}, will be:

$$\Delta L_{sc}^{2rms} = \frac{2Qc}{\sqrt{3} I_A \gamma'^2 R^2} f(A, \gamma_f) \tag{7}$$

Taking again $Q = 15$ pC, $E_0 = 100$ MV/m and $R = 1$ mm at S-band, one finds $\Delta L_{sc}^{2rms} = 17\,\mu$m for a long multi-cell gun ($\gamma_f \gg 1$), in absence of any phase-compression effect, i.e. at $\phi = 90°$ RF. It is interesting to note that Eq. (7) retains the same scaling ($1/R^2$) as the one typical of the surface charge regime, since the function $f(A, \gamma_f)$ saturates quickly at the value log(2) for $A > 1$: this is mainly due to the fact that the most relevant contribution to the bunch lengthening comes from the first stage of the acceleration (at low γ), that is, from the surface charge effects. For this reason, we have reduced by a factor 2 the quantity ΔL_{sc}^{2rms}, since the effective accelerating gradient close to the cathode is at least twice the average γ' [14]: the gradient decreases with oscillations down to $\gamma' = \alpha k \sin\phi$ in the following cells. Taking an average enhancement factor of $\sqrt{2}$ for the effective γ' implies a reduction by a factor 2 of ΔL_{sc}^{2rms} with respect to ΔL_{sc} in Eq. (6).

As far as the exit energy γ_f is high enough, one should not expect any further bunch lengthening: in other words, if the bunch has entered the linear charge regime at the gun exit (i.e. $A/\gamma_f \ll 1$), the following drift space down to the injection into the experimental area will not produce any significant extra lengthening from space charge effects. In

the opposite case, the effect of the residual longitudinal space charge must be taken into account: with a similar calculation as for Eq. (6), we found the bunch lengthening ΔL_d induced by a drift space of length z_d traveled in the surface charge regime

$$\Delta L_d = 2Qcz_d^2/(\sqrt{3}I_A\gamma_f^3R^2) \tag{8}$$

which gives $\Delta L_d = 26\ \mu$m after $z_d = 0.5$ m for $\gamma_f = 9$ and $R = 2$ mm (which are typical beam exit conditions for a 1 + 1/2 cell RF gun at S-band and $E_0 = 100$ MV/m). As clearly indicated by these scaling laws, the overall bunch lengthening induced by space charge effects is minimized for long multi-cell RF guns, which are able to produce exit energies high enough to freeze the residual space charge field.

Unfortunately, the scaling of space charge effects versus the cathode spot size R and the accelerating field γ', as shown in Eq. (6), is just opposite to that of single particle dynamics effects obtained in Eq. (4): in absence of any compensation for these effects, one should perform a trade-off in order to minimize the overall bunch lengthening by optimizing the two free parameters R and γ'.

A most powerful and effective mechanism to control the bunch lengthening is the phase-compression effect, which takes place in the first stage of the acceleration (typically the first cell of the RF gun) and it is basically due to a single damped synchrotron oscillation around a stable or an unstable point of the RF bucket, depending on the injection phase.

It can be shown [7] that for accelerating phases located off crest below $\pi/2$, i.e. for $\varphi < \pi/2$, the phase slippage $\Delta\varphi$ decreases with φ, indicating that particles emitted at different φ_0 will tend to move closer to each other, while at $\varphi > \pi/2$ they will tend to move far apart. As a result, the phase separation between two different photo-electrons emitted at two launching phases will follow the law

$$\Delta\lambda = 1 - \frac{\cot\varphi}{\alpha\sin\varphi}\left[\frac{1}{2} + \frac{1}{3\alpha\sin\varphi}\right] \tag{9}$$

where $\Delta\lambda$ represents the relative change in the phase-distance between the two electrons from the emission up to the relativistic motion at the gun exit. In absence of space charge effect, the bunch length L_{ex} at the gun exit will be given by $L_{ex} = L_{2rms}\,\Delta\lambda$, where L_{2rms} is the rms length of the laser pulse. The agreement between the analytical prediction and the numerical simulations has been shown to be quite excellent in the range $65° < \phi < 130°$, while for lower phases Eq. (9) is no longer capable to predict the even stronger phase-compression effect which occurs when the electrons are emitted at injection phases ϕ_0 close to 0° (i.e. when the electric field at the cathode is almost negligible).

In order to enhance the analytical model for the phase compression we include the space charge de-bunching effect by simply adding the term given by Eq. (7) and expressing the total (RF + space charge) change Δ of the electron bunch length L_{ex}, when extracted from the RF gun, in units of the laser pulse length L_{rms}, that is $\Delta = L_{ex}/L_{2rms}$. $\Delta > 1$ means a global de-bunching which can be caused by both RF and space charge, while $\Delta < 1$ means that the phase-compression effect from the RF is dominant over the space charge de-bunching. Substituting from Eqs. (7) and (9), we find

$$\Delta = 1 + \frac{1}{(\alpha\sin\phi)^2} \times\left[\frac{\chi}{\sqrt{3}kL_{rms}}f(A,\gamma_f) - \frac{\alpha}{2}\cos\phi - \frac{1}{3}\cot\phi\right] \tag{10}$$

where the dimensionless constant χ is the space charge field with the same normalization as α and represents the ratio $\chi = E_\sigma/E_\lambda$ between the surface space charge field at the cathode $E_\sigma = Q/2\pi\varepsilon_0R^2$ and the normalizing RF field $E_\lambda = mc^2k/e$. χ can also be expressed as $\chi = 2Qc/I_AkR^2$.

In order to check the simple analytical model, we derived also a 1D semi-analytical treatment, which can provide quickly, by simple numerical integration, some predictions over the entire operating range. These can be further validated by sophisticated, but long-lasting, numerical simulations.

The model is actually a simple two-slice, representing the bunch located at the head and the tail of a uniformly charged cylinder of radius R and nominal length L_0 (the rms length is again $L_{2rms} = L_0/\sqrt{3}$, which is equated to the 2σ of the Gaussian laser pulse length).

The equations for the phases (ϕ_t, ϕ_h) and energies (γ_t, γ_h) of the (tail, head) slices are as given by Ref. [7] with incorporation of the space charge term:

$$\begin{cases} \dfrac{d\gamma_t}{d\bar{z}} = 2\alpha\cos[\bar{z}]\sin[\varphi_t + \bar{z}] - \chi\left[1 + \dfrac{A}{\gamma} - \sqrt{1 + \dfrac{A^2}{\gamma^2}}\right] \\ \dfrac{d\gamma_t}{d\bar{z}} = 2\alpha\cos[\bar{z}]\sin[\varphi_h + \bar{z}] + \chi\left[1 + \dfrac{A}{\gamma} - \sqrt{1 + \dfrac{A^2}{\gamma^2}}\right]; \\ \gamma = \dfrac{\gamma_t + \gamma_h}{2} \\ \dfrac{d\varphi_t}{d\bar{z}} = \dfrac{\gamma_t}{\sqrt{\gamma_t^2 - 1}} - 1 \qquad \dfrac{d\varphi_h}{d\bar{z}} = \dfrac{\gamma_h}{\sqrt{\gamma_h^2 - 1}} - 1 \end{cases} \tag{11}$$

where $\bar{z} = kz$, $A = R/L_0 = R/\sqrt{3}L_{2rms}$.

In practical units, $\chi = 1.68Q[\text{nC}]/(R^2[\text{mm}]\nu_{RF}[\text{GHz}])$. Eq. (11) depends on three parameters: α, characterizing the acceleration in the RF field, plus A and χ, which describe the space charge field. The bunch length L is calculated by integrating Eq. (11) and setting $L = (\phi_t - \phi_h)/k$. The initial conditions at the cathode surface are $(\gamma_t = \gamma_h = 1)$ and $(\phi_{t0} = \phi_0 + kL_0/2,\ \phi_{h0} = \phi_0 - kL_0/2)$, where ϕ_0 is the RF phase when the center of the laser pulse hits the cathode.

It is interesting to evaluate at $\gamma \gg 1$, i.e. when the space charge term as well as the synchrotron motion are completely damped, the quantity $L/L_0 = (\phi_t - \phi_h)/(kL_0)$, which represents the relative lengthening (or compression, if smaller than 1) of the bunch with respect to the nominal length L_0, in analogy with Δ in Eq. (10).

The predicted values for Δ are plotted in Fig. 2 as a function of the accelerating phase ϕ (in radians), again for a long (10 + 1/2 cell) RF gun operated at S-band with $E_0 = 100$ MV/m, extracting a 15 pC bunch charge for three different laser pulse lengths L_{2rms}, namely 25, 50 and 100 μm. As clearly shown, the analytical (solid line) predictions of Eq. (10) are pretty close to the results derived by integrating Eq. (11), as far as the accelerating phase ϕ is not smaller than 0.9 and the bunch lengthening can be considered as perturbative, i.e. Δ is not too far from 1, which is indeed the assumption under which the analytical treatment has been developed.

It is also shown that, in this particular case, only the 100 μm pulse can be operated in such a way that the phase-compression effect can compensate completely, or even over compensate, the space charge de-bunching, producing values for Δ smaller than 1. It should be noticed, however, that both these evaluations assume a constant radius bunch accelerated through the gun, since they neglect the RF ponderomotive focusing as well as any other external focusing which may vary the bunch spot size. Moreover, it is well known that the transient RF kick in the first half-cell of the gun is capable to strongly de-focus the beam, together with the transverse space charge defocusing effects, in such a way that the beam radius in the following cells are typically twice the laser spot size at the cathode [14]. Since the space charge de-bunching, which is concentrated in the first cell, scales roughly as $1/R^2$, the predictions of such constant radius models are supposed to be over-estimating the real bunch lengthening effects, so that it is reasonable to assume that the numerical simulations will predict bunch lengthening roughly smaller by a factor 2 than the analytical ones.

It is interesting to represent, over an operating diagram, the capability of the phase-compression mechanism to compensate space charge de-bunching. For this we plot, as shown in Fig. 3, the roots of the equation $\Delta = 1$, as functions of α and ϕ, for fixed bunch charge $Q = 15$ pC, transverse normalized beam spot size $kR = 0.06$, and three different laser pulse lengths, $L_{2rms} = 25$, 50 and 100 μm. The dotted lines in Fig. 3 give the roots of $\Delta = 1$ at some representative aspect ratios (namely $A = 1$, 5, 10, 20) for a 25 μm bunch, while the solid lines are for a 50 μm bunch and the dashed for a 100 μm bunch (with the same set of aspect ratios). The thick solid line marks the transition between the forbidden region (below the line) and the region corresponding to possible values for the accelerating phase ϕ: recalling the relation between ϕ and the injection phase ϕ_0, i.e. $\phi = \phi_0 + 1/(2\alpha \sin\phi) + 1/6\,(\alpha \sin\phi)^2$, it is evident that for too low values of ϕ no positive values of ϕ_0 exist as solutions of the equation.

The comparison with the results obtained from Eq. (11) are reported at some points in the diagram, at $\alpha = 1.23$ ($E_0 = 75$ MV/m at S-band, $A = 23$ for 25 μm, $A = 11.5$ for 50 μm and $A = 5.8$ for 100 μm, respectively), at $\alpha = 1.64$ ($E_0 = 100$ MV/m at S-band), at $\alpha = 2.46$ ($E_0 = 150$ MV/m at S-band). The arrows mark the difference between analytical and semi-analytical predictions (analytical ones are located at the initial point of the arrow). The crosses mark the results of semi-analytical prediction derived at $\phi_0 = 0°$, for which we observed that no compensation is possible, that means $\Delta > 1$. Since the compensation effect is maximum at $\phi_0 = 0°$, this implies that $\Delta > 1$ at all phases. Again, the agreement between the analytical prediction and the numerical integration of Eq. (11) is quite satisfactory, within an error of 0.1 radian in ϕ, so that Eq. (10) can be used to evaluate at first order the

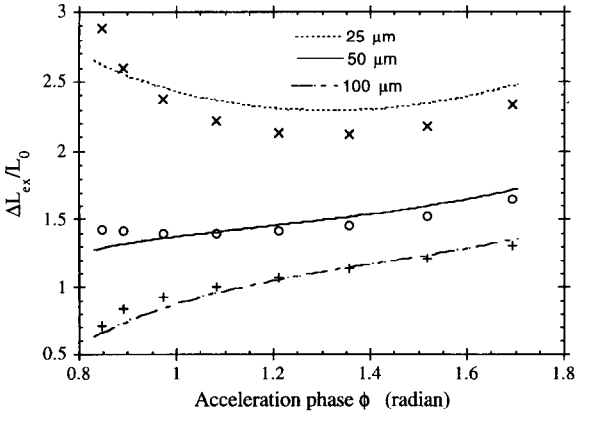

Fig. 2. The total change of electron bunch length at acceleration phase for a 10 + 1/2 cell RF gun: $E_0 = 100$ MV/m, $f_0 = 2.856$ Hz, $Q = 15$ pC.

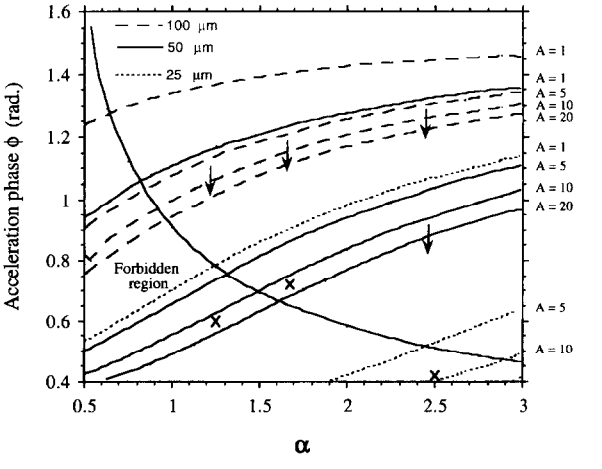

Fig. 3. An operating diagram to show the capability of the phase-compression for three different laser pulse lengths.

performances of a RF gun for the direct production of ultra-short electron bunches.

These performances, based mainly on the phase-compression mechanism, as clearly shown in Fig. 3, are enhanced at higher α, where shorter bunches and higher aspect ratios can be compensated. A more careful optimization should predict whether an operation with longer laser pulses over-compensated by the phase-compression may be in principle better than the operation of shorter pulses with complete or even partial compensation, in order to reach the minimum attainable bunch length.

Another important issue to be investigated is the possibility to compensate properly the tails in the photo-emission due to delayed time response of the photo-cathode material to the laser light.

3. Numerical simulation

The analysis in the previous section indicates that there is stretch of bunch length for acceleration and transportation of sub-picosecond electron beams. This bunch lengthening occurs mainly when the beam energy is low. To quantitatively characterize the performance of an RF photoinjector in the sub-picosecond regime, two possible schemes based on the UCLA plane wave transformer (PWT) linac [17,18] are investigated by numerical simulation. One is to use the present SATURNUS [19] setup: an RF photoinjector plus the PWT linac, with a drift space in between. Another is to use the PWT linac as a multi-cell RF photoinjector. The beam dynamics in the two cases is simulated using both PARMELA and ITACA [20]. The results from the two numerical codes are in good agreement. In all the simulation presented here, a laser pulse duration (FWHM) of 166 fs with a Gaussian distribution is assumed as well as an instantaneous response of the cathode. The total electron charge in a bunch is assumed to be 15 pC.

The PWT linac is a novel RF structure. It has been developed at UCLA [21]. This linac consists of seven full cells and two half cells with a total length of forty two centimeters. It is a standing wave RF linac operating at π mode. The UCLA PWT linac has many advantages, such as high impedance, high efficiency, and simplicity in fabrication, over commonly used RF structures. The coupling between individual cells in a PWT is achieved through a plane wave running back and forth in the structure. Therefore, each individual cell is coupled to every other cell. The neighbor cell coupling coefficient in the PWT is about 0.17. This strong coupling between cells makes this structure insensitive to mechanical errors. In addition, the ratio of maximum surface field to the axis peak field for the PWT is about 1.2 (the commonly used structures have a ratio higher than 2, which gives the PWT the capability to operate at high acceleration gradient. Recent high power operation at UCLA demonstrated that the PWT linac is a reliable and robust structure [21].

For an ultra-short electron bunch, the longitudinal space charge effect, as discussed in previous section, is significant at low energy even for a beam charge of 15 pC. This longitudinal self-field will induce bunch lengthening in the drift space from the gun exit to the linac. However, if we illuminate the cathode at such a phase that the electrons at the head of the bunch exiting from the RF gun have a lower energy than those at the tail, a bunching process will occur in the drift space. In this way, the debunching due to the longitudinal space charge effect could be, at least partially canceled. The optimal injection phase will depend upon the acceleration gradient of the RF gun and the distance of the drift section.

The layout for the first scheme is shown in Fig. 4. The RF gun is a widely used BNL-type $1\frac{1}{2}$-cell structure [22]. It can accelerate electrons to an energy of about 4 MeV. A solenoid magnet is used to provide focusing and match the beam parameters to the acceptance of the linac. The back solenoid is used to cancel the magnetic field on the cathode. The drift space between the RF gun and the linac is about 50 cm, which provides room for diagnostics. To propagate the beam to the experimental area, additional external focusing elements after the linac have to be used. The beamline after the linac is excluded from the simulation.

The acceleration gradient of the RF gun is set at 100 MV/m, which is at the upper limit of the normal operation of the RF gun. We assume the peak field on the axis of the PWT linac is 70 MV/m. Fig. 5 shows the

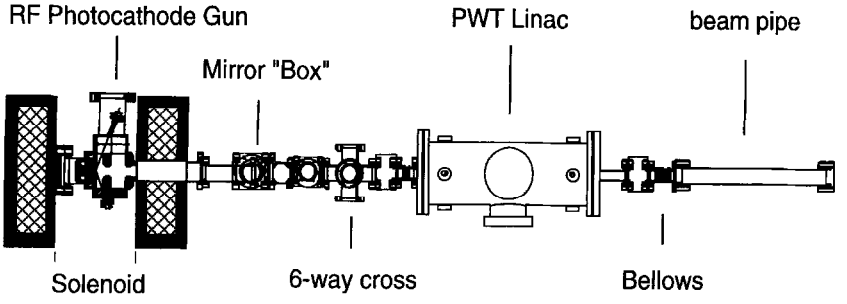

Fig. 4. Schematic set-up for option one: RF gun plus a PWT linac.

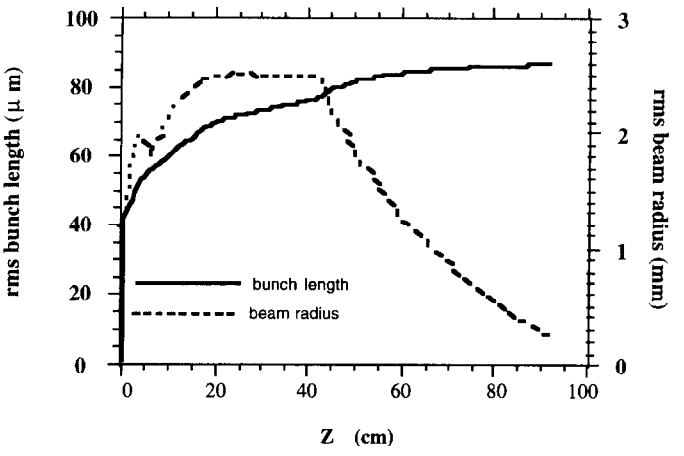

Fig. 5. Bunch length (FWHM) and beam spot size variations along the beamline for lunch phase 70°.

variation of the twice rms bunch length and the rms beam size along the beamline, up to exit of the linac for injection phase at 70°. It is seen that the bunch length stretches by about 50% before entering to the linac. This number is in good agreement with the analysis we made in previous sections, if we add contributions from both the slippage in the RF gun and longitudinal space charge effects. The acceleration of the RF linac induces additional debunching of about 20%. The injection phase into the linac is adjusted to achieve a maximum energy gain. The total beam energy is 18.5 MeV. The rms normalized emittance, which is shown in Fig. 6, along with the energy spread, at the linac exit is about 0.45 mm-mrad with an energy spread of about 0.1%. However, at a low injection phase, the bunch length will be reduced due to the RF bunching effects, which partially cancel the de-bunching due to the longitudinal space charge field. The sacrifice at low injection phase is

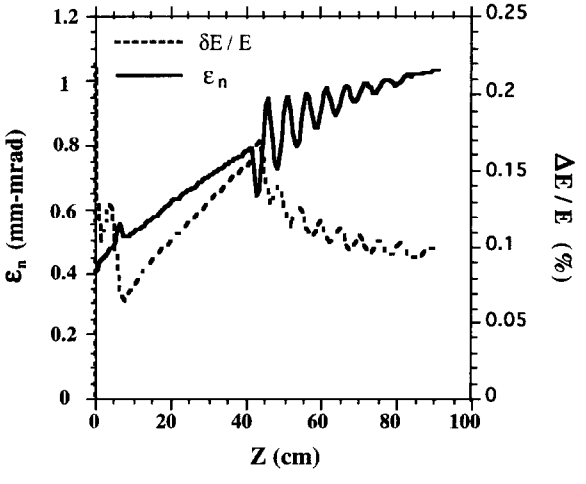

Fig. 6. Normalized emittance and energy spread variations along the beamline for lunch phase 70°.

that the transverse emittance will increase, which should still meet the requirements for most experiments. To minimise the transverse effects on the bunch length, the solenoid magnet amplitude is carefully adjusted to get a nearly constant beam size in the drift space. The focusing in the PWT linac is mainly due to the RF field. By optimizing the solenoid design, the transverse emittance can be further improved.

Another alternative is to use the PWT linac as a multi-cell RF gun. The advantage for this scheme is its simplicity and compactness. In addition, the elimination of the drift space between the gun and the linac should preserve the bunch length. With a properly designed solenoid magnet, the transverse focusing of the beam down to experimental area can be achieved without additional focusing components placed after the linac. Fig. 7 shows the set-up schematic of a multi-cell PWT RF photoinjector. Several solenoid magnets [23] are used to obtain a smooth focusing channel and minimize the transverse beam spot size. The bucking-coil is used for eliminating the magnetic field on the cathode.

The peak field on the cathode is 75 MV/m, same as that in other cells. The bunch length variation along the beamline is shown in Fig. 8 for an injection phase 35°. The significant bunch lengthening is seen to occur in the first half cell due to the strong space charge force, as discussed in previous section. Starting from the first full cell, the bunch is frozen by the accelerating RF field. After exiting from the PWT linac, the electrons have an energy of about 14 MeV, where the space charge effect is not significant. The final bunch length increases by about 20%. The rms beam size is also shown in Fig. 8. It is seen that the beam size can be focused down to as small as 40 μm (rms). By adjusting the solenoid magnet, we can focus the beam down to experimental area without additional focusing elements if it is not far away from the linac exit [10].

The phase compression at low injection phase is also

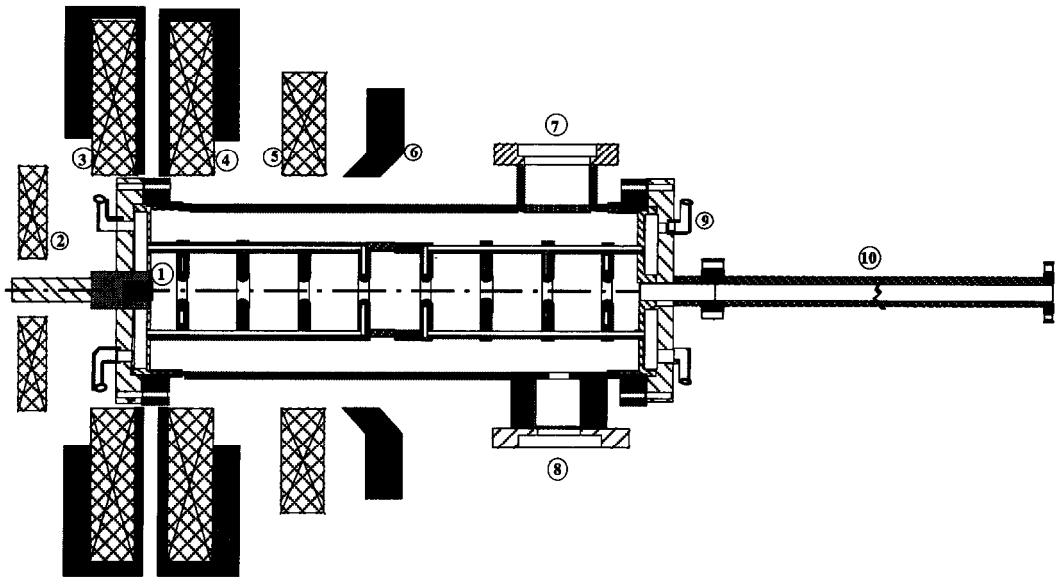

Fig. 7. Option two schematic: PWT multi-cell RF gun with solenoid magnets.

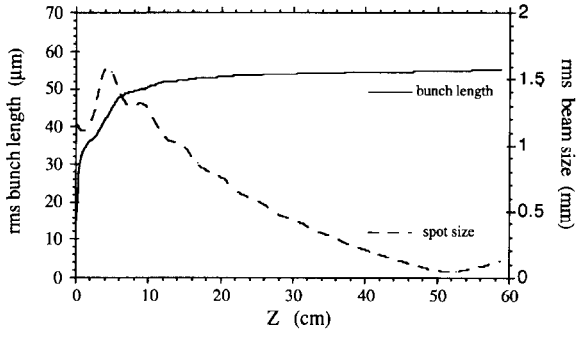

Fig. 8. The rms bunch engtth (FWHM) and beam size (FWHM) variation from the multi-cell PWT RF gun at a lunch phase of 30°.

true in a multi-cell RF injector. Fig. 9 shows the total bunch length and the normalized emittance at different injection phase. It is seen that a lower injection phase significantly reduces the bunch length stretch and also the beam energy with a slight increase of the emittance. At low injection phase, electrons emitted from the cathode at a later time receive higher acceleration than those emitted earlier. The higher energy electrons then keep catching up with those at the head and reduce the bunch length. The bunching effects and the space charge force compete with each other. As a result, there exists an optimized injection phase at which the bunch length is at a minimum. For the parameters we used in the simulation, the optimized injection phase is around 10° with a final bunch length of

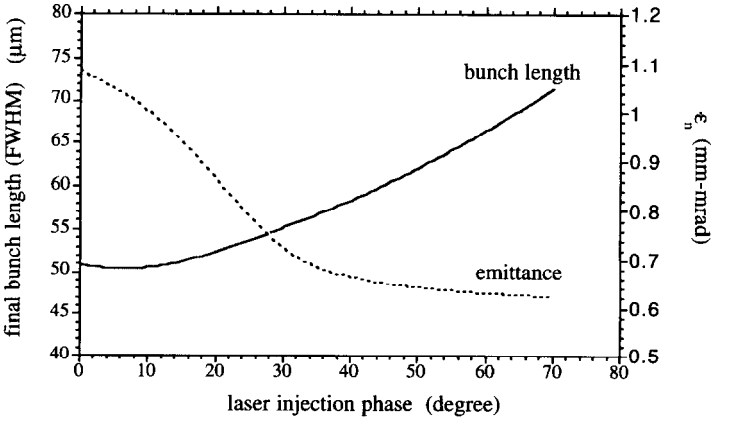

Fig. 9. The rms bunch length and rms normalized emittance from the PWT RF gun for different lunch phases.

55 μm at the linac exit. A higher bunch charge will increase the optimized injection phase and also produces a longer bunch.

4. Conclusion

The results that we have obtained show that it is possible to produce sub-picosecond electron bunch by RF photoinjectors, if the cathode response is short enough. In particular, the multi-cell PWT photoinjector is more simple for obtaining both short bunch length and small beam spot size, which simplifies beam transportation. The good beam quality from such a RF photoinjector can be used for many experiments where a short bunch length and a small emittance are needed, as for instance in the production of sub-picosecond X-ray pulses by Compton backscattering, or for injection into a plasma beatwave accelerator.

Acknowledgments

The authors wish to thank C. Clayton, C. Joshi and J. Rosenzweig for useful discussions. This work is supported by the US DOE Grants DE-FG03-92ER-40693 and INFN, Italy.

References

[1] C. Joshi et al., AIP Conf. Proc. 279 (1993) 379.
[2] F. Amiranoff et al., AIP Conf. Proc. 279 (1993) 411.
[3] H. Wiedemann, P. Kung and H.C. Lihn, Nucl. Instr. and Meth. A 319 (1992) 1.
[4] J. Rosenzweig et al., Pulse Compression in Photo Injectors: Applications to Advanced Accelerators, Proc. Int. Workshop on 2nd Generation Plasma Accelerators, Kardamyli, Greece (1995).
[5] L.M. Young, private communication, LANL (1995).
[6] T. Katsouleas et al., A Plasma Klystron for Generation Ultra-short Electron Bunches, Proc. Int. Workshop on 2nd Generation Plasma Accelerators, Kardamyli, Greece (1995).
[7] L. Serafini, Micro-bunch production with RF photo-injectors, Proc. Int. Workshop on 2nd Generation Plasma Accelerators, Kardamyli, Greece (1995).
[8] C. Pellegrini et al., Proc. Int. Workshop on 2nd Generation Plasma Accelerators, Kardamyli, Greece (1995).
[9] S. Hendrickson and J. Cary, Adiabatic Beam Bunching for Plasma Accelerators, Proc. Int. Workshop on 2nd Generation Plasma Accelerators, Kardamyli (1995).
[10] L. Serafini, R. Zhang and C. Pellegrini, Proc. Electron Micro Bunch Workshop, Brookhaven National Laboratory, New York (1995).
[11] C. Travier, Nucl. Inst. and Meth. A 340 (1994) 26.
[12] R. Brogle et al., Studies of Linear and Nonliner Photoelectric Emission for Advanced Accelerator Applications, Proc. Particle Accel. Conf., Dallas (1995).
[13] L. Serafini, Nucl. Instr. and Meth. A 340 (1994) 40.
[14] L. Serafini, Particle Accelerators 49 (1995) 253.
K.J. Kim, Nucl. Instr. and Meth. A 275 (1989) 201.
[15] P. Schoessow et al., submitted to Particle Accelerator Conf., Dallas, May (1995).
[16] The bunch generation distributed in time and the interaction with its image charge are two effects which tend to cancel each other: this is the main reason why the model described in Ref. [14], which adopts the same assumption, is very successful in the prediction of the space charge effects.
[17] D.A. Swenson, Proc. European Particle Accelerator Conf., 2, Rome, Italy, ed. S. Tazzari (1988) 1418.
[18] R. Zhang et al., Study of a novel compact standing wave RF linac, Nucl. Instr. and Meth., to be published.
[19] S. Hartman et al., Proc. of the 1991 Particle Accel. Conf., San Francisco (1991).
[20] L. Serafini and C. Pagani, Proc. 1st EPAC, Rome (1988).
[21] R. Zhang et al., Initial Operation of the UCLA Plane Wave Transformer (PWT) Linac, Proc. Particle Accel. Conf., Dallas (1995).
[22] J. Rosenzweig et al., Nucl. Instr. and Meth. A 341 (1944) 379.
[23] E. Colby, private communication.